







Detection of Simulated Periapical Lesion in Intraoral Digital Radiography with Different Brightness and Contrast

 Hugo GAËTA-ARAUJO,  Eduarda Helena Leandro NASCIMENTO,  Danieli Moura BRASIL,  Amanda Farias GOMES,  Deborah Queiroz FREITAS,  Christiano DE OLIVEIRA-SANTOS

ABSTRACT

Objective: To assess the detection of simulated periapical lesions in digital intraoral radiography with different levels of brightness and contrast combinations, and to investigate the observers' preference of image quality for this diagnostic task.

Methods: Digital radiographs were acquired prior to periapical lesion simulation and after each one of four defects enlargement. Original images were adjusted in 4 brightness and contrast combinations. Five observers evaluated the images according to the presence of periapical lesion on a 5-point scale. In a second moment, the observers ordinated the images subjectively, according to quality, from the best to the worst to detect the bone defect. The area under the receiver operating characteristic curve was calculated for the diagnostic values and compared by two-way ANOVA. The significance level was set at 5% ($P < 0.05$).

Results: No differences were found between the diagnostic values of the five combinations of brightness and contrast ($P > 0.05$). The overall results showed low values of area under the Receiver Operating Characteristic (ROC) curve and sensitivity of the periapical radiography in the detection of periapical lesions of sizes from 1 to 3, which rose substantially in size 4. For image quality, combinations with the lowest brightness and highest contrast were preferred by the observers in 58% of the cases.

Conclusion: Brightness and contrast adjustments do not influence the detection of simulated periapical lesions in digital intraoral radiography. Lower brightness and higher contrast images were preferred for this diagnostic task.

Keywords: Digital radiography, dental, diagnostic imaging, endodontic diagnosis, periapical lesions

Please cite this article as:

Gaêta-Araujo H, Nascimento EHL, Brasil DM, Gomes AF, Freitas DQ, de Oliveira-Santos C. Detection of Simulated Periapical Lesion in Intraoral Digital Radiography with Different Brightness and Contrast. *Eur Endod J* 2019; 3: 133-8

From the Department of Oral Diagnosis (H.G.A. ✉ hugogaeta@hotmail.com, E.H.L.N., D.M.B., A.F.G., D.Q.F.) Division of Oral Radiology, Piracicaba Dental School, University of Campinas UNICAMP, Piracicaba Sao Paulo, Brazil; Department of Stomatology (C.O.S.), Public Oral Health and Forensic Dentistry, Division of Oral Radiology, School of Dentistry of Ribeirao Preto, University of Sao Paulo USP, Sao Paulo, Brazil

Received 18 April 2019,
Accepted 17 September 2019

Published online: 22 November 2019
DOI 10.14744/eej.2019.46036

This work is licensed under a Creative Commons Attribution-NonCommercial 4.0 International License.



HIGHLIGHTS

- Adjustment of brightness and contrast do not influence periapical lesion diagnosis.
- Brightness and contrast can be adjusted according to individual preference.
- Images with lower brightness and higher contrast are preferred for periapical lesion diagnosis.

INTRODUCTION

Radiolucent periapical lesions (PL) usually arise as an inflammatory reaction in the periapical tissue because of microbial invasion to the root canal, as consequence of extensive caries (1) or dental trauma (2, 3), in addition to other non-odontogenic lesions. The detection of PL in radiographic

images is an important guide to the dental practitioners who may need to perform additional specific examinations (such as pulp sensibility tests) to confirm a given diagnosis that may require root canal treatment or other treatment options if the lesion is not related to the dental pulp. Therefore, an accurate PL diagnosis is critical for treatment planning.

Evaluation of periapical tissues in radiographic images is indispensable for the detection of inflammatory lesions of dental origin, as well as for monitoring the periapical status after endodontic therapies. Although cone beam computed tomography (CBCT) presents a high accuracy in the diagnosis of PL (4, 5), a greater dose of ionizing radiation is used, therefore, periapical radiographs are still the first-choice imaging exams for initial patient evaluation (6).

With the continuous advances in digital radiology in dentistry, image enhancement resources have been increasingly exploited in an attempt to improve the performance of radiographs in various diagnostic tasks (7–10). Some image tools have been tested for the evaluation of periapical bone tissues, with varying results for radiographic subtraction (11), contrast and sharpness

filter (8), inversion (12) and grey-scale and filtering treatment functions (13, 14). Although the tools for adjusting brightness and contrast are commonly used by clinicians and radiologists during the interpretation of digital radiography (10), the possible influence of different degrees of this adjustment on the detection of PL remains unclear.

Therefore, the purpose of this study was to determine whether the use of different brightness and contrast adjustments in digital radiographic images interferes with the detection of PL of different sizes. Additionally, the subjective preference of the observers regarding the degree of brightness and contrast for the evaluation of the periapical status was investigated.

MATERIALS AND METHODS

Sample selection and preparation

This study was approved by Institutional Review Board (protocol CAAE. 66971517.4.0000.5418). Initially, CBCT scans of seven posterior segments of dry human mandibles were acquired using a Picasso Trio unit (Vatech, Gyeonggi-Do, Republic of Korea) with acquisition parameters of 85 kVp, 5 mA, and voxel size of 0.2 mm. Six mandibular premolars (single-rooted) and four mandibular molars (double-rooted) without pre-existing periapical defects were selected. Buccal and lingual cortices width were measured on cross-sectional reconstructions at the level of the apex of those teeth (Fig. 1), to verify relevant differences in cortical thickness that could influence the image on the periapical radiographs. After CBCT examination, the selected teeth were carefully extracted. The floor of the 14 dental sockets were inspected with a dental operating microscope (DFV SA Microscopio, Sao Paulo, Brazil) to confirm that they remained intact after extraction.

Teeth were then repositioned in their sockets for the acquisition of periapical radiographs. A control group consisted of radiographs from dental sockets without PL. For the subsequent ra-

diographic acquisitions, teeth were removed from their position and PL were simulated by perforating the base of the dental socket with long-necked surgical spherical drills and high-speed handpiece, with the aid of a cavity preparation machine (15). The diameter and depth of the first defect were standardized at 1 mm, with size #2 drill. Three successive enlargements of the defects were performed, with #4 (1.4 mm), #6 (1.8 mm), and #8 (2.3 mm) drills. After each one of the defects enlargements, CBCT examination of the mandibles were acquired to assure that the PL simulation was confined into the trabecular bone. Radiographs were acquired for each PL size with the teeth reinserted in their corresponding sockets. A total of 70 radiographs were acquired (control +4 defect sizes, for each of the 14 dental sockets).

Image acquisition

Radiographic images were obtained with a CMOS sensor (Digora Toto system, Soredex, Tuusula, Finland), and a Focus (Instrumentarium, Tuusula, Finland) x-ray source operating at 70kVp, 7mA and exposure time of 0.063s. Before the study, three oral radiologists, working in consensus, evaluated initial images obtained with a range of exposure times (0.02s to 0.50s). Following the "as low as diagnostically acceptable" (ALADA) principle, the smallest exposure time able to produce images with enough quality for dental evaluation, was selected.

An acrylic device was used to hold the mandibles positioned to reproduce parallelism technique (40 cm focus-receptor distance and projection angulations). A wax cast was made for each mandibular segment to standardize its position between the radiographic acquisitions. A 2.5-cm-thick acrylic plate was placed between the mandible and x-rays source to simulate soft tissue coverage. To standardize initial brightness and contrast of images, all radiographs were acquired with an aluminium step wedge, with 8 steps of 2 mm thickness.

Image preparation and assessment

Grey values of the step wedge were measured using Image J software (National Institutes of Health, Bethesda, MD, USA),

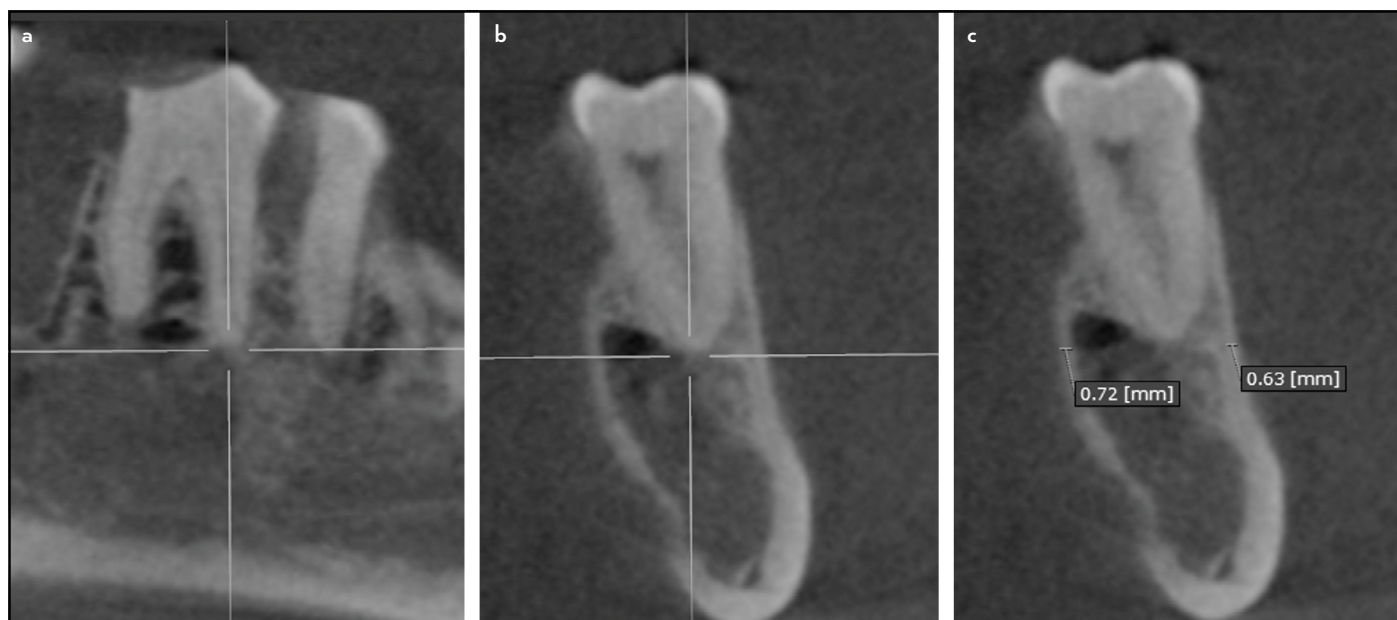


Figure 1. CBCT images representing cortical measures to avoid bias regarding its influence on PL detection. Images were reoriented according to the long-axis of the tooth (a), and measures were done immediately below the dental socket plane (b), in both buccal and lingual cortical plates (c)

to standardize image brightness and contrast as proposed by Nascimento et al. (16).

After standardization, each radiograph had brightness and contrast adjusted with aid of PowerPoint brightness/contrast tool (Microsoft Corporation, Redmond, WA, USA), in 4 different combinations, resulting in 5 different images for each radiograph acquired (i.e. initial +4 adjustments): C1 -30% brightness and +30% contrast; C2 -15% brightness and +15% contrast; C3 original image; C4 +15% brightness and -15% contrast; and C5 +30% brightness and -30% contrast (Fig. 2). Compression of images was disabled to maintain image quality. Thus, a total of 350 final images were randomized for assessment in JPEGView software (www.jpegview.sourceforge.net). For each radiograph, observers had to evaluate the presence of PL in a 5-point scale: (1) absent PL; (2) probably absent PL; (3) uncertain; (4) probably present PL; (5) present PL.

Subsequently, a PowerPoint presentation was prepared for subjective observer preferences analysis. Each original radiograph and its variations, except for the control group, were arranged side by side on a single slide with black background in a random sequence. Observers were then asked about their preference regarding the combination of brightness and contrast for visualization of the simulated PL and ordered images from "best" to "worst".

Both objective and subjective evaluations were performed independently by 5 oral radiologists with no previous knowledge of the image adjustment settings, in dimmed-lit condition, with a 24.1 inches LCD display with resolution of 1920X1200 pixels (Barco N.V., Courtrai, Belgium). Image enhancement tools use was not allowed. Observers assessed a maximum of 25 images

per day and had an interval of at least 3 days between image assessment sessions to avoid visual fatigue and observer learning. After 30 days of the end of the evaluations, 30% of the sample was re-assessed to calculate intraobserver agreement.

Statistical analysis

Data were analysed in SPSS version 22.0 software (IBM Corp, Armonk, NY, USA). The values of the mandibular cortices thickness measured in CBCT images were compared between molar and premolar regions by t-test. Intra and interobserver agreements were calculated by weighted Kappa test (<0.00, poor; 0.00-0.20, slight; 0.21-0.40, fair; 0.41-0.60, moderate; 0.61-0.80, substantial; 0.81-1.00, almost perfect) (17). The area under the ROC (Receiver Operating Characteristic) curve was calculated along with its 95% confidence interval to represent a point estimate of diagnostic accuracy. The ROC curve is a plot of test sensitivity (y coordinate) vs. its false positive rate (i.e., 1-specificity; x coordinate), and it has been used to assess diagnostic tests performances in radiology using scales with five (or more) categories. The area under the ROC curve translate the combination of the test sensitivity and specificity in different cut-off points, and therefore it measures the overall performance (i.e. accuracy) of the diagnostic test. The values of the area under the ROC curve varies between 0 and 1, and the bigger this value, the better is the diagnostic test performance. Sensitivity and specificity values were also obtained. Diagnostic values were compared by two-way ANOVA (brightness and contrast combinations x defect sizes), with Tukey post-hoc test. The level of significance was set at P<0.05.

RESULTS

Mean mandibular cortical thickness was 1.86 mm (±0.42) and 1.63mm (±0.74) for premolar and molar regions respectively,

TABLE 1. Intra and interobserver agreement values for detection of periapical lesion distributed according to the brightness and contrast combinations

Brightness and contrast combinations	Intraobserver agreement		Interobserver agreement	
	Mean	(Min.-Max.)	Mean	(Min.-Max.)
C1 (-30% brightness; +30% contrast)	0.24	(-0.14-0.54)	0.06	(-0.12-0.27)
C2 (-15% brightness; +15% contrast)	0.41	(0.24-0.69)	0.00	(-0.28-0.17)
C3 (original image)	0.45	(0.38-0.5)	0.28	(0.01-0.55)
C4 (+15% brightness; -15% contrast)	0.30	(0.01-0.53)	0.26	(0.09-0.63)
C5 (+30% brightness; -30% contrast)	0.37	(0.12-0.61)	0.29	(-0.07-0.61)

C1 to C5: Combinations of brightness and contrast 1 to 5, Min: Minimum, Max: Maximum

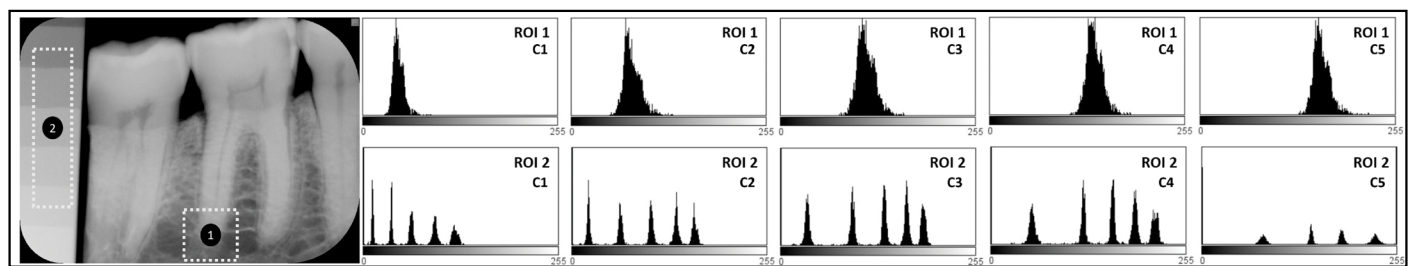


Figure 2. Representation of the histograms in each adjustment of brightness and contrast (C1 to C5). On the left, a radiograph demonstrating two selected regions of interest (ROI) for histogram measure: ROI 1-on the periapical region of the tooth; ROI 2-on the aluminum step wedge used to standardize images. The upper set of histograms represents ROI 1 and the lower set represents ROI 2. It is possible to observe the influence that the brightness and contrast adjustments have on the histogram, shifting the gray values to the right as the brightness increases (C1 to C5) and stretching the values as the contrast increases (C5 to C1)

TABLE 2. Mean values and standard deviations for the area under the receiver operating characteristic curve, sensitivity and specificity for each periapical lesion size and brightness and contrast combinations tested

Diagnostic values	PL size	Brightness and contrast combinations				
		C1	C2	C3	C4	C5
Az	Size 1	0.55 (0.04) Aa	0.57 (0.06) Aa	0.57 (0.07) Aa	0.55 (0.06) Aa	0.56 (0.03) Aa
	Size 2	0.64 (0.08) Aab	0.63 (0.09) Aa	0.62 (0.04) Aab	0.60 (0.10) Aab	0.61 (0.08) Aa
	Size 3	0.63 (0.09) Aab	0.63 (0.08) Aa	0.64 (0.06) Aab	0.58 (0.08) Aab	0.62 (0.05) Aa
	Size 4	0.70 (0.06) Ab	0.71 (0.11) Aa	0.72 (0.07) Ab	0.71 (0.08) Ab	0.65 (0.09) Aa
Sensitivity	Size 1	0.43 (0.17) Aa	0.44 (0.13) Aa	0.43 (0.21) Aa	0.44 (0.22) Aa	0.46 (0.22) Aa
	Size 2	0.56 (0.19) Aa	0.56 (0.15) Aa	0.50 (0.25) Aa	0.56 (0.19) Aa	0.54 (0.23) Aa
	Size 3	0.51 (0.20) Aa	0.56 (0.19) Aa	0.56 (0.21) Aa	0.46 (0.16) Aa	0.56 (0.06) Aa
	Size 4	0.66 (0.17) Aa	0.61 (0.23) Aa	0.67 (0.25) Aa	0.66 (0.20) Aa	0.56 (0.22) Aa
Specificity*	All sizes	0.70 (0.15) Aa	0.69 (0.19) Aa	0.69 (0.19) Aa	0.74 (0.21) Aa	0.60 (0.21) Aa

PL: Periapical lesion, C1 to C5: Combinations of brightness and contrast 1 to 5, Az: Area under the receiver operating characteristic curve. Different letters (uppercase horizontally and lowercase vertically) differ from each other according to Two-way ANOVA. *Only one value of specificity is shown for each brightness/contrast variation because the same control group is used, therefore, the number of true negative cases are the same for all periapical lesion sizes

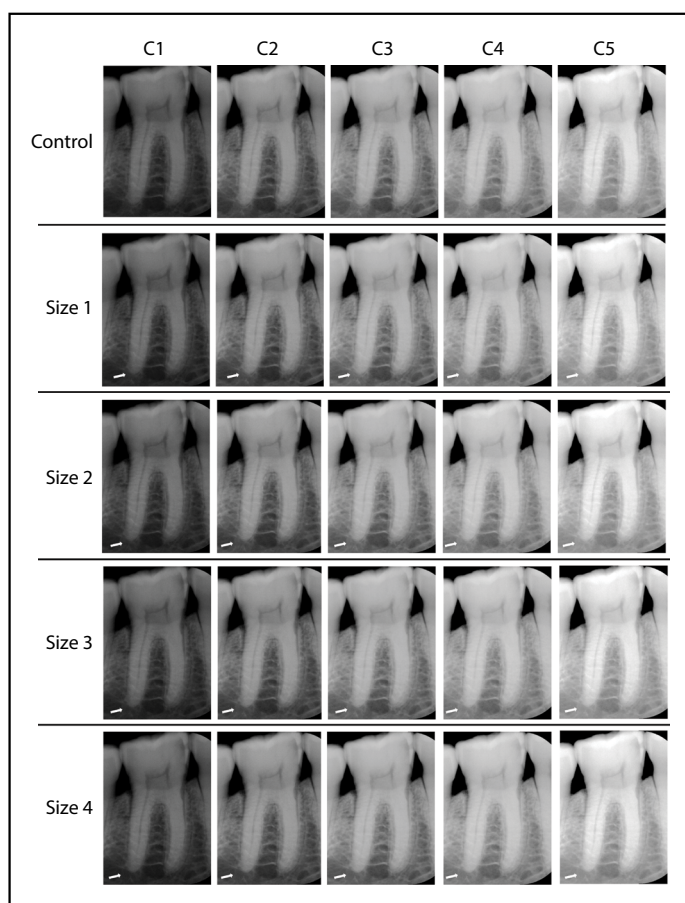


Figure 3. Radiographic images showing the same tooth (arrows) prior (control group) and after the simulation of apical bone defects of different sizes (Size 1 to Size 4), arranged according to the brightness and contrast variations (C1, -30% brightness; +30% contrast; C2, -15% brightness; +15% contrast; C3, original image; C4, +15% brightness; -15% contrast; C5, 30% +brightness; -30% contrast)

without statistically significant difference ($P=0.353$). Intra and interobserver agreements are shown in Table 1. The highest

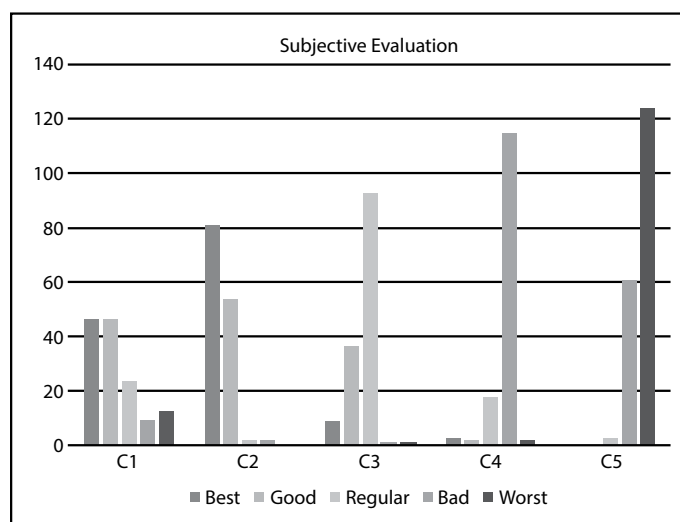


Figure 4. Observers' subjective preference for detection of PL distributed according to brightness and contrast adjustments of digital radiographs

mean values for intraobserver agreement was found for C3 and C2 (moderate reproducibility), while the other variations showed fair reproducibility. There was a slight interobserver agreement for C1 and C2, and fair for C3, C4 and C5.

Table 2 summarizes the diagnostic values related to detection of the different PL distributed according to the combinations. No significant differences were found in diagnostic values among the five brightness/contrast variations ($P>0.05$). When comparing the smallest (size 1) with the largest (size 4) PL, overall diagnostic values are slightly higher for larger defects. Such difference is statistically significant only for the area under the ROC curve (Az) and in some image brightness/contrast combinations (C1, C3, and C4).

According to the subjective image quality for this diagnostic task (Figs. 3 and 4), the C2 variation was preferred by the observers, being classified as "best" in 58% of the cases, fol-

lowed by C1 variation (32.9% of the cases). The original image (C3) was marked as regular most of the cases, while the adjustments with higher brightness and lower contrast (C4 and C5) were considered "bad" and "worst" in 82.1% and 89.3%, respectively.

DISCUSSION

Image enhancement available in digital radiography potentially improves image quality. The use of image filters have been described in the literature (7, 18, 19) and mostly does not show significant influence on diagnosis (7, 20, 21). Depending on the digital imaging system used, the application of filters may be time-consuming or complicated (13). On the other hand, brightness and contrast adjustments can easily be done in any image software and they are usually preferable (7, 13). Normally these adjustments are done according to personal visual preferences, however, our proposal was to standardize image brightness and contrast adjustments in five different pre-set combinations, so it would be possible to assess if these enhancements interfere on the diagnosis of PL.

Mean accuracy of digital periapical radiography for the detection of PL in the present study ranged between 0.55 and 0.72 (depending on the defect size and brightness/contrast combination), which is accordance with previous studies, which reported accuracies from 0.26 to 0.87 (1, 4, 22–27). Considering PL size, the largest defects yielded higher sensitivity and accuracy than the smallest defects, as expected (1, 5).

Simulation of PL with burs does not reproduce all the details and potential variations in radiographic presentation of these lesions. However, it has been extensively used in *in vitro* studies (1, 5, 22, 26) since it allows the observation of different lesion sizes, a greater sample, and multiple image acquisitions (21). Other proposed methodology for the PL simulation is through acid-induced demineralization of the bone tissue (24, 25, 28). The choice of using controlled perforation of the bone was due to the standardization of the cavities size, allowing more reliable comparisons of the accuracy considering the different sizes of PL. The acid-induced process cannot control defect size (3).

The simulated defects of our samples were made only on trabecular bone, which has been associated with lower detection rates compared to defects reaching cortical bone (1). Minimal bone resorptions are disguised due to image overlapping, which is inherent to conventional imaging techniques (1). This limitation can be solved by three-dimensional imaging (CBCT). Studies comparing both techniques reported higher accuracy for CBCT (1, 4, 5, 22, 24), however, along with CBCT advantages comes a higher radiation dose for the patient and expenses. For this reason, CBCT is indicated only in cases where conventional radiographs fail to provide valid information when there are contradictory clinical signs and symptoms (6).

In a previous study, Kullendorff and Nilsson (13) evaluated the detection of simulated PL lesions on a direct digital radiography system with and without the use of post-processing tools that allowed grey-scale and filtering adjustments. The authors concluded that the image processing did not increase the overall diagnostic accuracy for the detection

of PL. Posteriorly, this same research group compared the performance of conventional and digital radiographs (with and without brightness and/or contrast adjustments) in the diagnosis of natural periapical lesions, and found higher accuracy for conventional film than for digital radiography with post-processing (14). This result can be attributed to the fact that the 'gold standard' for its periapical lesions was based on the conventional radiographic images, which were evaluated by an experienced observer. In addition, the degree of the brightness and contrast adjustment of digital images was not controlled, and the digital system used is currently outdated (14). Recently, an *in vitro* study (26) assessed the influence of enhancement filters on diagnosis of PL and found no influence of these filters for this diagnostic task. However, lesions with greater sizes were more detectable, regardless of the post-processing method (21).

When registering the most used post-processing tools during the assessment of periapical status (including the function of changing the grey scale and applying filters such as sharpening, edge enhancement and smoothing), Kullendorff and Nilsson (13) found that the images with lower brightness and higher contrast levels were preferred by the observers. In the present study, the preferable images for PL evaluation were C1 and C2 variations, which presented lower brightness and higher contrast, as well. Despite the observers' preference, our data did not show any difference in accuracy values between the range of brightness and contrast variations tested, which may be related to the theory that the diagnosis of trabecular bone lesions initially depend more on the detection of structural changes than on the perception of density changes (14). It means that image adjustment might be done as the observer feels more comfortable and secure.

In clinical scenario, patient's signs and symptoms help practitioners to identify conditions that may lead to PL (e.g. pulpal necrosis or unsuccessful root canal treatments). But in some cases, this pathological condition may be silent and only detected accidentally during radiographic examination. More studies are needed to evaluate the impact of other enhancement tools, or the combinations of these tools, on the diagnosis of PL.

CONCLUSION

In conclusion, brightness and contrast enhancements, within the range of combinations tested in the present study, do not interfere on the diagnosis of PL and can be used according to the observer's preference. Lower brightness and higher contrast images were preferred for this diagnostic task.

Disclosures

Conflict of interest: None declared.

Ethics Committee Approval: Piracicaba Dental School Review Board (protocol CAAE. 66971517.4.0000.5418).

Peer-review: Externally peer-reviewed.

Financial Disclosure: This work was supported by the Coordenação de Aperfeiçoamento de Pessoal de Nível Superior - Brasil (CAPES) under grant Finance Code 001.

Authorship contributions: Concept – H.G.A., E.H.L.N.; Design – H.G.A., E.H.L.N., D.M.B., A.F.G.; Supervision – D.Q.F., C.O.S.; Funding – H.G.A., E.H.L.N., D.M.B., A.F.G.; Materials – E.H.L.N., A.F.G.; Data collection &/or processing – H.G.A., E.H.L.N., D.M.B., A.F.G.; Analysis and/or interpretation – H.G.A., E.H.L.N., D.M.B., A.F.G., D.Q.F., C.O.S.; Literature search – H.G.A., E.H.L.N., D.M.B., A.F.G.; Writing – H.G.A., E.H.L.N., D.M.B., A.F.G.; Critical Review – D.Q.F., C.O.S.

REFERENCES

- Patel S, Dawood A, Mannocci F, Wilson R, Pitt Ford T. Detection of periapical bone defects in human jaws using cone beam computed tomography and intraoral radiography. *Int Endod J* 2009; 42(6):507–15. [CrossRef]
- Raghav N, Reddy SS, Giridhar AG, Murthy S, Yashodha Devi BK, Santana N, et al. Comparison of the efficacy of conventional radiography, digital radiography, and ultrasound in diagnosing periapical lesions. *Oral Surg Oral Med Oral Pathol Oral Radiol Endod* 2010; 110(3):379–85. [CrossRef]
- Petersson A, Axelsson S, Davidson T, Frisk F, Hakeberg M, Kvist T, et al. Radiological diagnosis of periapical bone tissue lesions in endodontics: a systematic review. *Int Endod J* 2012; 45(9):783–801. [CrossRef]
- de Paula-Silva FW, Wu MK, Leonardo MR, da Silva LA, Wesselink PR. Accuracy of periapical radiography and cone-beam computed tomography scans in diagnosing apical periodontitis using histopathological findings as a gold standard. *J Endod* 2009; 35(7):1009–12. [CrossRef]
- Campello AF, Gonçalves LS, Guedes FR, Marques FV. Cone-beam computed tomography versus digital periapical radiography in the detection of artificially created periapical lesions: A pilot study of the diagnostic accuracy of endodontists using both techniques. *Imaging Sci Dent* 2017; 47(1):25–31. [CrossRef]
- European Commission. Radiation Protection No 172. Cone beam CT for dental and maxillofacial radiology (Evidence-based guidelines). Available at: http://www.sedentext.eu/files/radiation_protection_172.pdf. Accessed Sep 24, 2019.
- Raitz R, Assunção Junior JN, Fenyo-Pereira M, Correa L, de Lima LP. Assessment of using digital manipulation tools for diagnosing mandibular radiolucent lesions. *Dentomaxillofac Radiol* 2012; 41(3):203–10. [CrossRef]
- Choi JW, Han WJ, Kim EK. Image enhancement of digital periapical radiographs according to diagnostic tasks. *Imaging Sci Dent* 2014; 44(1):31–5.
- Peixoto LR, Gonzaga AK, Melo SL, Pontual ML, Pontual Ados A, de Melo DP. The effect of two enhancement tools on the assessment of the relationship between third molars and the inferior alveolar canal. *J Craniofac Surg* 2015; 43(5):637–42. [CrossRef]
- Rovaris K, de Faria Vasconcelos K, do Nascimento EH, Oliveira ML, Freitas DQ, Haiter-Neto F. Brazilian young dental practitioners' use and acceptance of digital radiographic examinations. *Imaging Sci Dent* 2016; 46(4):239–44. [CrossRef]
- Carvalho FB, Gonçalves M, Tanomaru-Filho M. Evaluation of chronic periapical lesions by digital subtraction radiography by using Adobe Photoshop CS: a technical report. *J Endod* 2007; 33(4):493–7. [CrossRef]
- de Molon RS, Morais-Camillo JA, Sakakura CE, Ferreira MG, Loffredo LC, Scaf G. Measurements of simulated periodontal bone defects in inverted digital image and film-based radiograph: an *in vitro* study. *Imaging Sci Dent* 2012; 42(4):243–7. [CrossRef]
- Kullendorff B, Nilsson M. Diagnostic accuracy of direct digital dental radiography for the detection of periapical bone lesions. II. Effects on diagnostic accuracy after application of image processing. *Oral Surg Oral Med Oral Pathol Oral Radiol Endod* 1996; 82(5):585–9. [CrossRef]
- Kullendorff B, Petersson K, Rohlin M. Direct digital radiography for the detection of periapical bone lesions: a clinical study. *Endod Dent Traumatol* 1997; 13(4):183–9. [CrossRef]
- Soares CJ, Fonseca RB, Gomide HA, Correr-Sobrinho L. Cavity preparation machine for the standardization of *in vitro* preparations. *Braz Oral Res* 2008; 22(3):281–7. [CrossRef]
- Nascimento EH, Gaëta-Araujo H, Vasconcelos KF, Freire BB, Oliveira-Santos C, Haiter-Neto F, et al. Influence of brightness and contrast adjustments on the diagnosis of proximal caries lesions. *Dentomaxillofac Radiol* 2018; 47(8):20180100. [CrossRef]
- Landis JR, Koch GG. The measurement of observer agreement for categorical data. *Biometrics* 1977; 33(1):159–74. [CrossRef]
- Wenzel A. A review of dentists' use of digital radiography and caries diagnosis with digital systems. *Dentomaxillofac Radiol* 2006; 35(5):307–14. [CrossRef]
- Wenzel A, Haiter-Neto F, Frydenberg M, Kirkevang LL. Variable-resolution cone-beam computerized tomography with enhancement filtration compared with intraoral photostimulable phosphor radiography in detection of transverse root fractures in an *in vitro* model. *Oral Surg Oral Med Oral Pathol Oral Radiol Endod* 2009; 108(6):939–45. [CrossRef]
- Belém MD, Tabchoury CP, Ferreira-Santos RI, Groppo FC, Haiter-Neto F. Performance of a photostimulable storage phosphor digital system with or without the sharpen filter and cone beam CT for detecting approximal enamel subsurface demineralization. *Dentomaxillofac Radiol* 2013; 42(5):20120313. [CrossRef]
- Brasil DM, Yamasaki MC, Santaella GM, Guido MCZ, Freitas DQ, Haiter-Neto F. Influence of VistaScan image enhancement filters on diagnosis of simulated periapical lesions on intraoral radiographs. *Dentomaxillofac Radiol* 2019; 48(2):20180146. [CrossRef]
- Stavropoulos A, Wenzel A. Accuracy of cone beam dental CT, intraoral digital and conventional film radiography for the detection of periapical lesions. An *ex vivo* study in pig jaws. *Clin Oral Investig* 2007; 11(1):101–6. [CrossRef]
- Estrela C, Bueno MR, Leles CR, Azevedo B, Azevedo JR. Accuracy of cone beam computed tomography and panoramic and periapical radiography for detection of apical periodontitis. *J Endod* 2008; 34(3):273–9.
- Sogur E, Baksı BG, Gröndahl HG, Lomcali G, Sen BH. Detectability of chemically induced periapical lesions by limited cone beam computed tomography, intra-oral digital and conventional film radiography. *Dentomaxillofac Radiol* 2009; 38(7):458–64. [CrossRef]
- Soğur E, Gröndahl HG, Baksı BG, Mert A. Does a combination of two radiographs increase accuracy in detecting acid-induced periapical lesions and does it approach the accuracy of cone-beam computed tomography scanning? *J Endod* 2012; 38(2):131–6. [CrossRef]
- Tsai P, Torabinejad M, Rice D, Azevedo B. Accuracy of cone-beam computed tomography and periapical radiography in detecting small periapical lesions. *J Endod* 2012; 38(7):965–70. [CrossRef]
- Leonardi Dutra K, Haas L, Porporatti AL, Flores-Mir C, Nascimento Santos J, Mezzomo LA, et al. Diagnostic Accuracy of Cone-beam Computed Tomography and Conventional Radiography on Apical Periodontitis: A Systematic Review and Meta-analysis. *J Endod* 2016; 42(3):356–64. [CrossRef]
- Ozen T, Kamburoğlu K, Cebeci AR, Yüksel SP, Paksoy CS. Interpretation of chemically created periapical lesions using 2 different dental cone-beam computerized tomography units, an intraoral digital sensor, and conventional film. *Oral Surg Oral Med Oral Pathol Oral Radiol Endod* 2009; 107(3):426–32. [CrossRef]